ACS MATERIALS Au
AN OPEN ACCESS JOURNAL OF THE AMERICAN CHEMICAL SOCIETY

pubs.acs.org/materialsau

Article

# Reinforced Polyphenylene Ionomer Membranes Exhibiting High Fuel Cell Performance and Mechanical Durability

Junpei Miyake, Takayuki Watanabe, Haruhiko Shintani, Yasushi Sugawara, Makoto Uchida, and Kenji Miyatake*

Cite This: *ACS Mater. Au* 2021, 1, 81–88

Read Online

ACCESS | Metrics & More | Article Recommendations | Supporting Information

**ABSTRACT:** We report on the preparation of reinforced membranes (SPP-QP-PE, where SPP stands for sulfonated polyphenylene), composed of an in-house proton-conductive polyphenylene ionomer (SPP-QP) and a flexible porous polyethylene (PE) mechanical support layer. By applying the push coating method, dense, uniform, transparent, and thin SPP-QP-PE membranes were obtainable. The use of SPP-QP with higher ion exchange capacity induced very high proton conductivity of SPP-QP-PE, leading to high fuel cell performance even at low humidified conditions (e.g., at 80 °C and 30% relative humidity), which had not been attainable with the existing reinforced aromatic ionomer membranes. The flexible porous PE substrate improved the mechanical toughness of the membranes; the elongation at break increased by a factor of 7.1 for SPP-QP-PE compared to that with the bare SPP-QP membrane, leading to mechanical durability at least 3850 wet−dry cycles under practical fuel cell operating conditions (the United States Department of Energy protocol). Overall, the reinforced aromatic ionomer membranes, SPP-QP-PE with balanced proton conductivity, mechanical toughness, and gas impermeability, functioned well in fuel cells with high performance and durability.

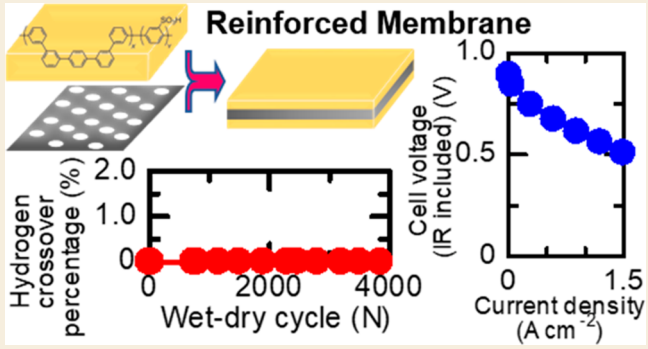


**KEYWORDS:** *push coating method, polyphenylene ionomer, porous polyethylene substrate, reinforced membranes, fuel cells*

## INTRODUCTION

Polyphenylenes are one of the simplest polymers, consisting solely of phenylene rings in the polymer backbones. Because of the robust and conjugated structure, polyphenylenes and their derivatives have found some applications in organic electronic devices, sensors, polymer film additives, fluorescent tags, nanocarriers, and proton exchange membrane fuel cells (PEMFCs).[1] Proton exchange membranes (PEMs) are one of the key components in fuel cells to play a vital role in transporting protons (and water) and avoid direct contact of hydrogen and oxygen.[2] Perfluorosulfonic acid (PFSA) polymer membranes (Nafion, for example) have been the benchmark PEMs due to their high mechanical/chemical stability, proton conductivity, and thin membrane toughness.[3] There is a need for alternative PEMs with gas barrier properties, thermal stability, low production cost, and environmental compatibility.[4−12]

Recently, sulfonated polyphenylenes or polyphenylene ionomer membranes have gained significant interest as alternative fluorine-free PEMs because of their high chemical stability in addition to their high gas impermeability, thermal stability, and potentially low production cost commonly expected for aromatic ionomer membranes. Fujimoto et al. reported that sulfonated phenylated poly(phenylene) (or sulfonated poly(phenylene) synthesized by Diels−Alder polymerization) membranes exhibited high thermal stability and high proton conductivity (~123 mS $cm^{-1}$ at 30 °C in liquid water) but insufficient tensile properties (elongation at break = 6% and Young's modulus = 0.28 GPa, in a wet state).[13] More recently, Holdcroft et al. proposed a structurally defined version of the sulfonated phenylated poly(phenylene) membranes, exhibiting high fuel cell performance at 80 °C and 100% relative humidity (RH) and durability in an open-circuit voltage (OCV) hold test, but still tensile properties (elongation at break = ~20.3%, Young's modulus = 0.151 GPa, tensile strength = ~7.7 MPa, in wet state) seemed insufficient.[14−16] We proposed a simpler polyphenylene ionomer membrane (SPP-QP, where SPP stands for sulfonated polyphenylene) that exhibited excellent chemical stability, gas impermeability, and proton conductivity, resulting in high fuel cell performance at 80 °C and low RH (e.g., 30% RH) and

Received: February 24, 2021
Published: April 26, 2021

durability in the OCV hold test (the average OCV decay during the testing was ~226 $\mu$V $h^{-1}$ for 1000 h at 80 °C and 30% RH ($H_2$/air)).[17] Similar to the other polyphenylene ionomer membranes, however, mechanical properties (elongation at break = 19%, Young's modulus = 1.1 GPa, maximum stress = 27 MPa) remained an issue. As PEMs experience severe mechanical stress in the operating fuel cell conditions (frequent humidity and/or current density changes), mechanical durability of polyphenylene ionomer membranes has to be improved.

One of the promising methods to enhance the mechanical durability of PEMs is to reinforce with more mechanically robust substrates. In fact, perfluorosulfonic acid (PFSA) polymers are reinforced with expanded polytetrafluoroethylene (PTFE) (e.g., GORE SELECT) in practical fuel cell applications. Giancola et al. reported that a PFSA polymer with short-side-chain (i.e., Aquivion)/electrospun polysulfone fiber web nanocomposite membranes exhibited enhanced mechanical properties and dimensional stability compared with their bare (or nonreinforced) counterparts at low fiber content (5 wt %), keeping high proton conductivity.[18] For nonfluorinated PEMs, Bonnet et al. reported that sulfonated poly(ether ether ketone) (sPEEK)-based composite membranes containing 10% amorphous silica, 30% zirconium phosphate, or 40% amorphous zirconium phosphate sulfophenylphosphonate presented high conductivities (0.03−0.09 S $cm^{-1}$) at 100 °C/100% RH.[19] Oh et al. reported that a sPEEK/boron nitride nanoflake (BNNF)/1-pyrenesulfonic acid (PSA) composite membrane (ion exchange capacity (IEC) = ~1.9 mmol $g^{-1}$) showed improved proton conductivity, tensile strength, and dimensional stability.[20] The composite membrane showed high fuel cell performance under high humidity conditions (i.e., at 80 °C and 100% RH) and improved mechanical durability (at 80 °C, 950 wet/dry cycles by the U.S. Department of Energy (USDOE) protocol) compared to those of the bare sPEEK membrane. Zhang et al. reported that a hydrocarbon polyelectrolyte/poly(vinylidene fluoride) (PVDF) blend membrane (IEC = 1.25 mmol $g^{-1}$) exhibited mechanical durability better than that of Nafion NRE211 under RH cycle tests (at 80 °C, 20,000 RH cycles for the blend membrane and ~6000 RH cycles for the Nafion NRE211 membrane by a protocol developed for automotive applications).[21] However, the blend membrane showed inferior fuel cell performance under moderately humidified conditions (i.e., at 80 °C and 50% RH) because of the low proton conductivity of the blend membrane. We reported a sulfonated polybenzophenone-based (SPK, in-house) membrane reinforced with nonwoven fabric (NF, composite of glass and polyethylene terephthalate (PET) fibers) (IEC = ~1.7−1.9 mmol $g^{-1}$) that exhibited improved in-plane dimensional stability, resulting in high mechanical durability (at 80 °C, 18,320 wet/dry cycles by the Fuel Cell Commercialization Conference of Japan (FCCJ) protocol) compared to that of the bare SPK membrane.[22] The NF-reinforced SPK membrane also showed good fuel cell performance under moderately humidified conditions (i.e., at 80 °C and 53% RH). Up to date, there have been no precedents on reinforced aromatic ionomer membranes that achieved both high fuel cell performance under lower humidity conditions (e.g., at 80 °C and 30% RH) and long-term mechanical durability.

To meet the challenge, we have designed a novel reinforced membrane (SPP-QP-PE) consisting of the polyphenylene ionomer (SPP-QP) as a highly proton-conductive and chemically stable PEM even at low humidity and a porous polyethylene (PE) substrate as a highly flexible mechanical support. To impregnate the SPP-QP into the pore of the PE substrate homogeneously throughout the membrane, a push coating method (pressure applied during the evaporation of cast solvents) was used.[23] The push coating method was originally developed for preparing uniform and thin organic semiconductor membranes on highly hydrophobic surfaces for flexible electronics.[23] By applying this method, a polar SPP-QP solution was homogeneously spread over nonpolar PE substrate, resulting in the formation of uniform, thin ionomer composite membranes. The preparation and properties including fuel cell performance and durability of the SPP-QP-PE membranes are discussed in details.

## EXPERIMENTAL METHODS

### Materials

The SPP-QP ionomer was prepared according to the literature (Table 1).[17] The porous substrate (SETELA PE9: thickness = 9 $\mu$m, porosity = 32%, pore size = 23 nm; SETELA PE7: thickness = 7 $\mu$m, porosity = 44%, pore size = 62 nm) was provided from Toray Industries, Inc.

**Table 1. Properties of the SPP-QP**

| | IEC (mmol $g^{-1}$) | | | molecular weight[a] (kDa) | | |
|---|---|---|---|---|---|---|
| SPP-QP | target[b] | NMR | titration[c] | $M_n$ | $M_w$ | $M_w/M_n$ |
| 1 | 3.1 | 2.4 | 2.3 | 49.5 | 190 | 3.83 |
| 2 | 4.8 | 3.8 | 3.9 | 45.8 | 163 | 3.57 |

[a]Determined by gel permeation chromatography (GPC). [b]Calculated from the feed monomer ratio. [c]Determined by acid−base titration.

### Preparation of the SPP-QP-PE Membrane

The reinforced membrane was prepared by the push coating method according to the literature.[23] As a typical example, 15 wt % dimethylsulfoxide (DMSO) solution of SPP-QP was placed on a flat glass plate (preirradiated with a UV lamp for 1 min), then spread with a Baker applicator (slit width of 76.2 $\mu$m). Into the solution, SETELA (preirradiated with UV lamp for 1 min on both sides) was impregnated. The UV irradiation (ORC manufacturing Co., Ltd., VUE-3020) was conducted to make the substrates hydrophilic and improve the compatibility of the solvents and substrates. Additional SPP-QP solution was placed on the top and then spread with a Baker applicator (slit width of 152 $\mu$m). Silicone sheet (1.0 mm thick, dimethylpolysiloxane, AS ONE Corporation) was placed on the top while preventing the entry of air bubbles (no additional pressure was applied other than the weight of the silicone sheet). After being dried at 40 °C for 12 h, the glass plate and the silicone sheet were removed. Then, the resulting reinforced membrane was immersed in 1 M sulfuric acid and DI water and dried to yield the targeted SPP-QP-PE membrane.

### Fuel Cell Operation

A commercial Pt/CB catalyst (1.9 g, Tanaka Kikinzoku TEC10E50E), DI water (8 g), and ethanol (15.7 g) were placed in 45 mL of a zirconia pot containing 20 zirconia balls ($\varphi$ = 5 mm), and the mixture was mixed using a Fritsch Pulverisette 6 planetary ball mill at 270 rpm for 30 min. To the mixture was added 5 wt % Nafion D-521 dispersion (14.4 g, IEC = 0.95−1.03 mmol $g^{-1}$, Du Pont), and the mixture was mixed using the planetary ball mill at 270 rpm for 30 min. The mass ratio (Nafion/C) was set at 0.70. A catalyst-coated membrane (CCM) was prepared by spraying the catalyst paste on both sides of the membrane using a Nordson pulse−swirl−spray apparatus. The resulting CCM was dried at 60 °C overnight and then hot-pressed at 140 °C and 10 kgf $cm^{-2}$ for 3 min. The geometric electrode area and the Pt loading amount in the catalyst layer were 29.16 $cm^2$ (5.4 cm × 5.4 cm) and 0.50 ± 0.05 mg $cm^{-2}$, respectively.


https://doi.org/10.1021/acsmaterialsau.1c00002
ACS Mater. Au 2021, 1, 81−88

The CCM was sandwiched by two SGL 29BC gas diffusion layers (GDL, 230 $\mu$m thick) and gaskets (200 $\mu$m thick) and mounted into a JARI (Japan Automobile Research Institute) standard cell, which had serpentine flow channels on both sides. Finally, a pressure of 10 kgf $cm^{-2}$ was uniformly applied to the electrode by tightening with a torque wrench. Linear sweep voltammetry (LSV) was measured to investigate the $H_2$ permeability of the membrane by monitoring the oxidation current of $H_2$ permeated from the anode to the cathode. During the LSV measurement, $H_2$ and $N_2$ were fed to the anode and the cathode at 100 mL $min^{-1}$, respectively. The cathode potential was swept from 0.15 to 0.6 V at a sweep rate of 5 mV $s^{-1}$. To obtain a polarization curve, pure $H_2$ and $O_2$ (or air) were fed to the anode and the cathode, respectively. The gas utilizations were 70% (anode) and 40% (cathode), respectively. The high-frequency resistance (HFR) was measured by utilizing a Tsuruga Electric ac milliohmmeter (model 3356) at 1.0 kHz.

### Wet–Dry Cycling Test

The membrane electrode assembly (MEA) for the wet–dry cycling test was prepared according to the literature.[24] A catalyst ink was prepared by mixing carbon-supported Pt–Ru anode material (TEC61E54, Tanaka Kikinzoku Kogyo K.K.) or Pt–Co cathode catalyst (TEC36E52, Tanaka Kikinzoku Kogyo K.K.), PFSA ionomer (EW = 909 g $equiv^{-1}$, Asahi Glass Co.) solution, water, and ethanol. A CCM was prepared by spraying the catalyst ink onto anode and cathode sides of the membrane. The geometric electrode area and the Pt loading amount in the catalyst layer were 36 $cm^2$ (6 cm × 6 cm) and 0.3 mg $cm^{-2}$ (anode) and 0.6 mg $cm^{-2}$ (cathode), respectively. The CCM was heated at 160 °C for 5 min and then sandwiched by two soft-type GDL (400 $\mu$m thick, ∼50% of porosity),[25,26] gaskets, and subgasket films (38 $\mu$m thick polyphenylene sulfide sheet). The MEA was mounted into a single-cell holder, which had two sets of single-serpentine carbon separators. Finally, the cell was fixed with a force of 10 kgf $cm^{-2}$. The wet–dry cycling test was conducted according to the USDOE protocol.[27]

To the anode and cathode were supplied hydrogen and nitrogen gases, respectively. Dry and wet (humidified at 90 °C) gases were prepared for both gas lines. During the mechanical durability testing, the dry and wet gases were switched every 2 min. The flow rates of the gas for the anode and cathode were both at 2 slm. The cell temperature and the dew points of the gases were 80 and 90 °C, respectively. The extent of the membrane degradation was monitored by quantifying the percentage of $H_2$ crossover through the membrane during the durability cycling. The percentage of $H_2$ crossover is defined as follows: HCO = $V_{H_2,cathode,outlet}/V_{H_2,anode,inlet}$ × 100, where $V_{H_2,anode,inlet}$ is the hydrogen flow rate measured at the inlet gas stream before being passed through the humidifier at 23 °C and 1 atm. $V_{H_2,cathode,outlet}$ is the hydrogen flow rate calculated by the $H_2$ percentage in the total outlet gas from the cathode. The percentage of $H_2$ in the cathode outlet gas was obtained as follows. Both the cell temperature and the dew points for the cathode and anode gases were set at 60 °C. Both the cathode and anode gas flow rates were set at 0.3 slm. The cathode outlet gas, including nitrogen, water, and hydrogen, was dehumidified by being passed through an ice bath. Then, an aliquot of 2 mL of gas was taken at ∼23 °C and 1 atm and was subjected to a Shimazu GC-8A gas chromatograph. The $H_2$ peak area in the GC was accumulated, and the $H_2$ percentage was calculated by calibration data (i.e., the area for the standard 1% $H_2$ gas). The percentage of hydrogen obtained from GC was equal to the percentage of $H_2$ in the cathode outlet gas after the dehumidification. The $V_{H_2,cathode,outlet}$ was obtained by multiplying the percentage of hydrogen and the cathode inlet flow rate.

## RESULTS AND DISCUSSION

### Preparation of Reinforced Membranes

The SPP-QP ionomer (Figure 1a, IEC = 2.4–3.8 mmol $g^{-1}$, determined by $^1$H NMR spectra) was synthesized according to the literature.[17] These ionomers possessed high solubility in organic solvents such as dimethylacetamide and DMSO (but not soluble in water) and high molecular weights (Table 1), providing thin membranes by the solution-casting method. A typical appearance of the SPP-QP membrane is shown in Figure 1b. Using the SPP-QP and a porous substrate (Figure 1c, Toray SETELA PE7 or PE9), the composite (or reinforced) membranes, SPP-QP-PE (Figure 1d), were prepared by the push coating method according to the literature (see the Experimental Methods for details).[23] In this method, pressure was applied during the evaporation of cast solvents; thus uniform, thin ionomer membranes were obtainable even when the affinity between the polymer (or SPP-QP with high polarity) and the porous substrate (or PE with low polarity) was not sufficient. In fact, a simple solution-casting method (i.e., SPP-QP solution was cast onto the PE substrate) resulted in inhomogeneous turbid composite membranes. SPP-QP-PE composite membranes prepared by the push coating method was highly transparent to the absence of light scattering from the pores, indicative of successful filling of the ionomer into the pores of the PE substrate.

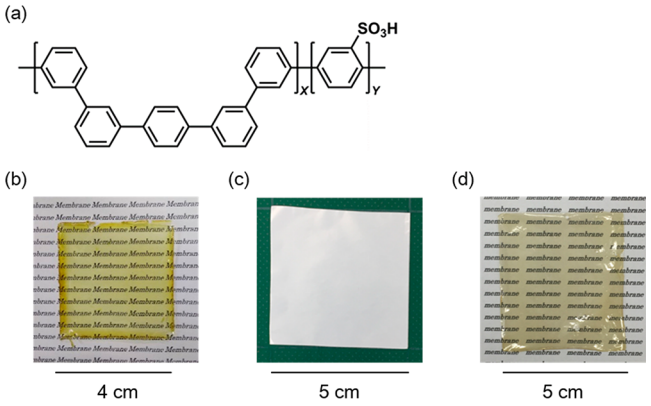


**Figure 1.** (a) Molecular structure of SPP-QP. Photos of (b) SPP-QP membrane, (c) porous substrate (SETELA PE7), and (d) reinforced membrane (SPP-QP-PE7).

Figure 2 shows a typical cross-sectional scanning electron microscopy (SEM) image of the SPP-QP-PE9 membrane, where a sandwich-like (triple-layer) structure (i.e., SPP-QP/

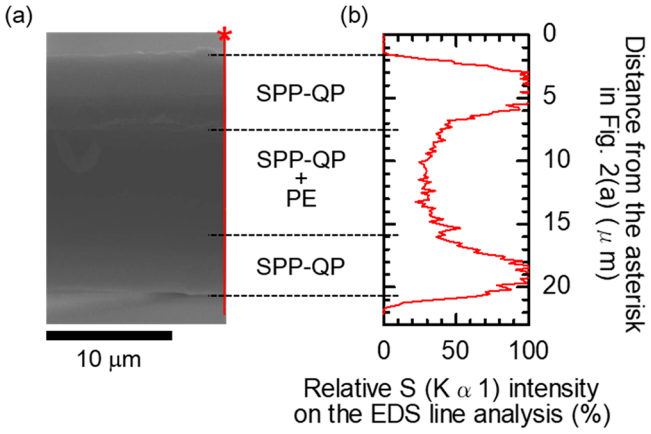


**Figure 2.** (a) Cross-sectional SEM image of the SPP-QP-PE9 membrane (SPP-QP with IEC = 2.4 mmol $g^{-1}$ was used). (b) Relative sulfur atom ($K_{\alpha 1}$) intensity on the EDS line analysis quantified by backscattered electrons as a function of the distance from the asterisk in panel a.


https://doi.org/10.1021/acsmaterialsau.1c00002
ACS Mater. Au 2021, 1, 81–88

SPP-QP + PE/SPP-QP) was confirmed. The middle layer (~8.3 μm thick) was the composite of SPP-QP and the PE substrate. Complete filling of the ionomer was also suggested by the homogeneous middle layer, with no pores left throughout the site. The top and bottom layers (~6.0 and 4.8 μm thick, respectively) did not contain the PE substrate but contained only the SPP-QP membrane. Energy-dispersive X-ray spectroscopy (EDS) also supported those structural analyses; the sulfur intensity was higher for the top and bottom layers (SPP-QP) and lower for the middle layer (SPP-QP + PE). Given that the maximum sulfur intensity of the SPP-QP layer was 100%, the average sulfur intensity of the middle layer was calculated to be 35%, which was in good accordance with the porosity of the PE substrate (32%), suggesting the successful formation of the SPP-QP-PE composite membrane. The IEC value of the SPP-QP-PE9 membrane obtained by titration was 1.8 mmol $g^{-1}$, in good accordance with the calculated IEC (1.9 mmol $g^{-1}$) from the polymer density, IEC, and the thickness of each layer. Hereafter, the calculated or titrated IEC values will be used for composite or bare SPP-QP membranes, respectively.

## Properties of Reinforced Membranes

To investigate the effect of the PE substrate on gas permeability, hydrogen and oxygen permeability was investigated at 80 °C and 30 to 90% RH (Figure 3). At 30% RH, the

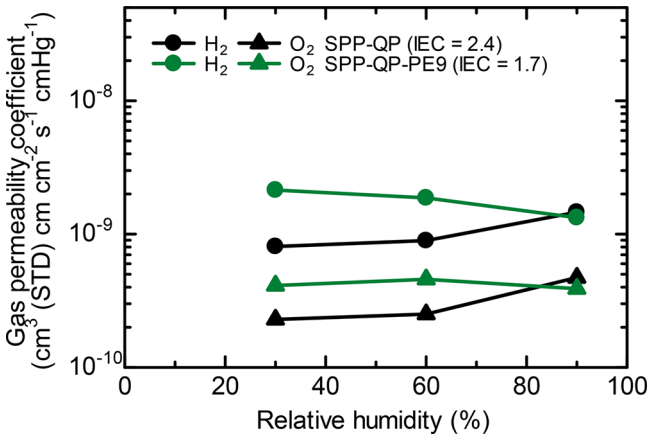


**Figure 3.** Humidity dependence of the hydrogen and oxygen permeability coefficient of the membranes at 80 °C. For the SPP-QP-PE9 (IEC = 1.7 mmol $g^{-1}$), SPP-QP with IEC = 2.4 mmol $g^{-1}$ was used.

$H_2$ and $O_2$ permeability coefficients of the SPP-QP-PE9 membrane were slightly higher than those of the SPP-QP membrane, probably because of the higher permeabilities of the hydrophobic PE substrate. With increasing humidity, the differences in the coefficients between the SPP-QP and SPP-QP-PE9 membranes became smaller, indicating that the swelling of SPP-QP was suppressed in the porous substrate. At 90% RH, the permeability coefficients were comparable for the bare and reinforced membranes. It should be noted that both the SPP-QP ($1.46 \times 10^{-9}$ $cm^3$ (STD) cm $cm^{-2}$ $s^{-1}$ $cmHg^{-1}$ or 14.6 barrer for hydrogen, $4.72 \times 10^{-10}$ $cm^3$ (STD) cm $cm^{-2}$ $s^{-1}$ $cmHg^{-1}$ or 4.72 barrier for oxygen, at 80 °C and 90% RH) and SPP-QP-PE9 ($1.33 \times 10^{-9}$ $cm^3$ (STD) cm $cm^{-2}$ $s^{-1}$ $cmHg^{-1}$ or 13.3 barrier for hydrogen, $3.90 \times 10^{-10}$ $cm^3$ (STD) cm $cm^{-2}$ $s^{-1}$ $cmHg^{-1}$ or 3.90 barrier for oxygen, at 80 °C and 90% RH) membranes exhibited permeability coefficients much lower than those ($7.35 \times 10^{-9}$ $cm^3$ (STD) cm $cm^{-2}$ $s^{-1}$ $cmHg^{-1}$ or 73.5 barrier for hydrogen, $3.15 \times 10^{-9}$ $cm^3$ (STD) cm $cm^{-2}$ $s^{-1}$ $cmHg^{-1}$ or 31.5 barrier for oxygen, at 80 °C and 90% RH) for the PFSA Nafion membrane.[17]

Figure 4 displays water uptake and proton conductivity of the membranes at 80 °C as a function of relative humidity. As a

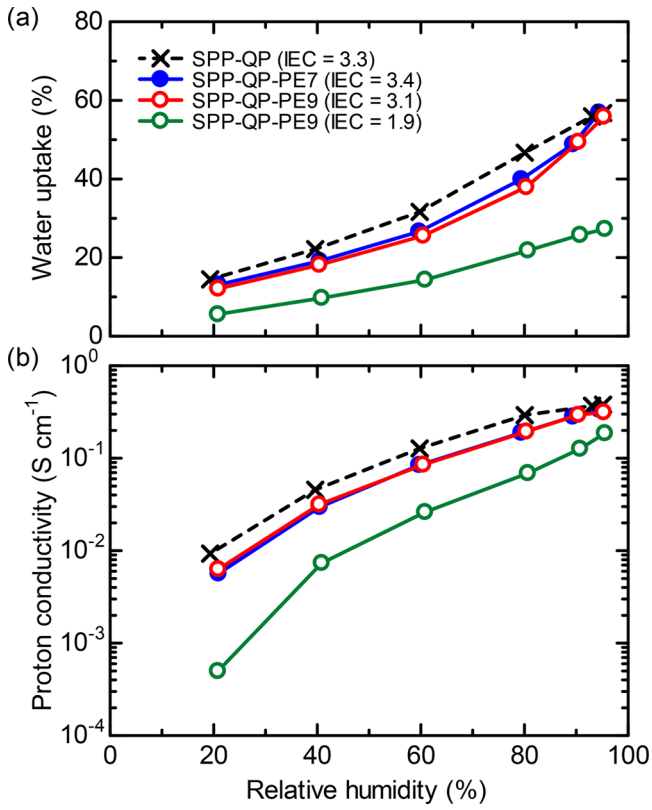


**Figure 4.** Humidity dependence of (a) water uptake and (b) proton conductivity of the membranes at 80 °C. For the SPP-QP-PE7 (IEC = 3.4 mmol $g^{-1}$), SPP-QP-PE9 (IEC = 3.1 mmol $g^{-1}$), and SPP-QP-PE9 (IEC = 1.9 mmol $g^{-1}$), SPP-QP with IEC = 3.8 mmol $g^{-1}$, IEC = 3.8 mmol $g^{-1}$, and IEC = 2.4 mmol $g^{-1}$ was used, respectively.

general trend, the water uptake and proton conductivity increased with increasing IEC value and humidity. In more detail, the proton conductivity and water uptake were replotted as a function of the IEC (Figure S1). Compared to SPP-QP and SPP-QP-PE-9 membranes, the SPP-QP-PE-7 membrane absorbed a slightly smaller amount of water, indicating that the porous PE7 substrate suppressed swelling of the ionomer, although the effect was not very significant. Similarly, the proton conductivity of the reinforced SPP-QP-PE7 membrane was slightly lower than that of the SPP-QP and SPP-QP-PE9 membranes. The SPP-QP (3.3 mmol $g^{-1}$) having the highest water uptake showed the highest proton conductivity at any humidity. Despite the presence of a nonconductive PE substrate, the SPP-QP-PE7 (3.4 mmol $g^{-1}$) and SPP-QP-PE9 (3.1 mmol $g^{-1}$) membranes showed reasonably high proton conductivity, suggesting that the proton and water transport pathway (e.g., the hydrophilic domain size determined by TEM image was approximately 3 nm in diameter for the SPP-QP (2.4 mmol $g^{-1}$) membrane[17]) was not impeded in the composite membranes because of much larger pore sizes (62 nm for PE7, 23 nm for PE9) of the PE substrate. This trend was similar to that of our previously


https://doi.org/10.1021/acsmaterialsau.1c00002
ACS Mater. Au 2021, 1, 81−88

reported nonwoven fabric reinforced aromatic ionomer membranes (NF-reinforced SPK).[22] The present approach (reinforcement of the high IEC ionomer with a porous substrate using the push coating method) was more advantageous for obtaining thinner, more proton-conductive reinforced membranes, in particular, at low humidity (e.g., 5.67 mS $cm^{-1}$ for SPP-QP-PE7 (3.4 mmol $g^{-1}$), 1.1 mS $cm^{-1}$ for the NF-reinforced SPK (1.69 mmol $g^{-1}$), at 80 °C and 20% RH).

Polyphenylene ionomer membranes are generally not mechanically tough with low ability to elongate due to high rotational barrier of the backbones composed of stiff phenylene groups. Figure 5 represents the stress−strain curves of the SPP-QP and reinforced membranes at 80 °C and 60% RH, and the related data are shown in Table 2. The maximum strain and stress of the SPP-QP membrane (3.0 mmol $g^{-1}$) were 19% and 27 MPa, respectively. The reinforced membranes exhibited much higher maximum strain. Specifically, the maximum strain increased by a factor of 7.1 for SPP-QP-PE7 (3.2 mmol $g^{-1}$) and 5.6 for SPP-QP-PE9 (1.8 mmol $g^{-1}$), compared to that of the bare SPP-QP membrane (3.0 mmol $g^{-1}$). The reinforcement lowered the Young's modulus slightly, whereas the maximum stress of the SPP-QP-PE membranes was comparable or even higher than that of the bare SPP-QP membrane. By lowering the humidity from 60 to 20−30% RH, the elongation at break of the SPP-QP-PE9 membrane became smaller by ∼50%, which was comparable with the bare SPP-QP membrane.[17] Then, the tensile test was suspended at the point of 107% of the strain for the SPP-QP-PE9 (3.1 mmol $g^{-1}$) membrane, and the recovered sample was subjected to the proton conductivity measurement. As shown in Figure S2, the recovered sample showed proton conductivity comparable to that of the original sample over a wide range of humidity, suggesting that the SPP-QP ionomer in the reinforced membrane did not break in the pores but deformed with the PE substrate probably because of interfacial interactions with the substrate in the nanopores.

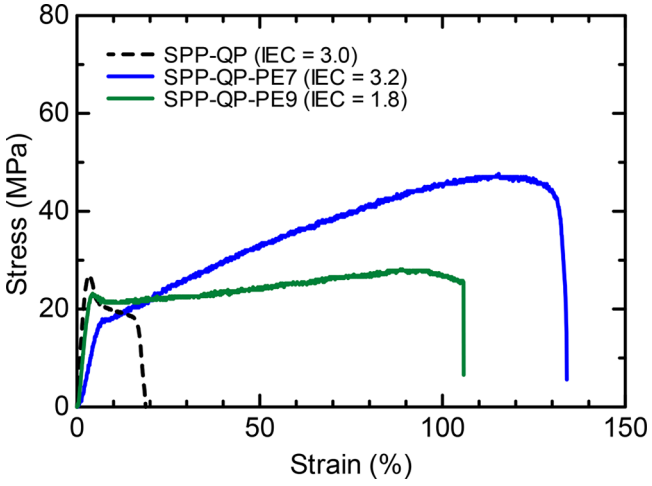


**Figure 5.** Tensile properties of the membranes at 80 °C and 60% RH. For the SPP-QP-PE7 (IEC = 3.2 mmol $g^{-1}$) and SPP-QP-PE9 (IEC = 1.8 mmol $g^{-1}$), SPP-QP with IEC = 3.8 mmol $g^{-1}$ and IEC = 2.4 mmol $g^{-1}$ was used, respectively.

**Table 2. Tensile Properties of the Membranes**

| sample | Young's modulus (GPa) | maximum stress (MPa) | maximum strain (%) |
|---|---|---|---|
| SPP-QP | 1.1 | 27 | 19 |
| SPP-QP-PE7 | 0.36 | 47 | 134 |
| SPP-QP-PE9 | 0.82 | 28 | 106 |

## Evaluation of Fuel Cell Performance and Wet/Dry Cycle Durability

Taking into account the balance of high proton conductivity, mechanical toughness, and water uptake, we selected the SPP-QP-PE7 membrane for fuel cell evaluation. Because of the mechanical stability, a thinner membrane was available for the SPP-QP-PE7 (12 $\mu$m thick) compared to the bare SPP-QP membrane (22 $\mu$m thick). To estimate the hydrogen permeation through the membrane in the cell, LSVs were measured by feeding $H_2$ to the anode and $N_2$ to the cathode, respectively, at 80 °C and 30% RH (Figure S3). The oxidation current density of the permeated $H_2$ from the anode to the cathode was 0.68 mA $cm^{-2}$ for the SPP-QP-PE7 membrane, whereas that for the bare SPP-QP membrane was 0.23 mA $cm^{-2}$, due to the slightly higher gas permeabilities and smaller thickness of the SPP-QP-PE7 membrane. It should be noted that the SPP-QP-PE7 cell showed lower oxidation current density (or lower hydrogen permeability) compared with that (1.38 mA $cm^{-2}$) for the Nafion NRE 211 membrane (25 $\mu$m thick), in spite of the smaller thickness of the SPP-QP-PE7 membrane.

Figure 6 represents the *IV* curves and ohmic resistance of the fuel cells at 80 °C ($H_2/O_2$). The OCV of the SPP-QP-PE7 cell at 100% RH was 0.98 V, which was slightly lower than that (1.0 V) of the SPP-QP cell, reflecting the slightly higher

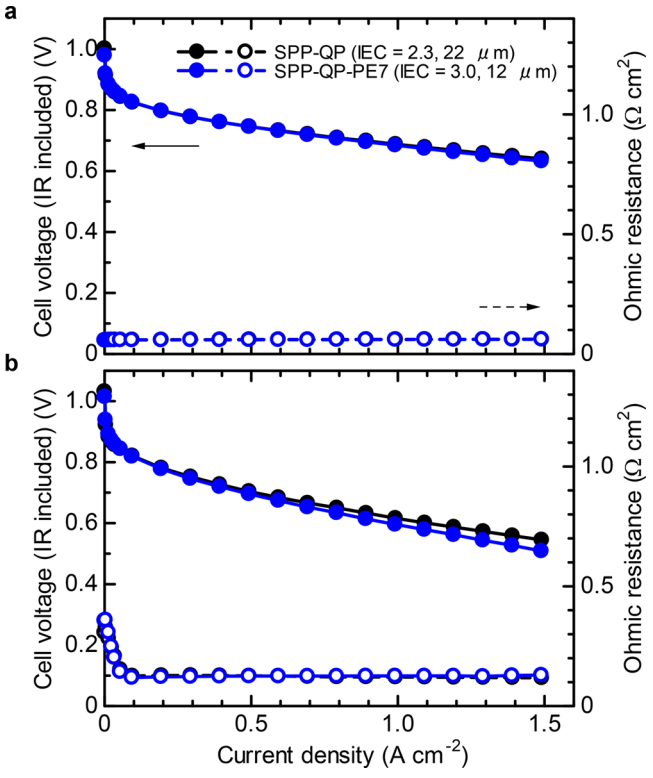


**Figure 6.** IR-included $H_2/O_2$ *IV* curves (solid symbols) and ohmic resistances (open symbols) of the fuel cells at 80 °C and (a) 100% RH and (b) 30% RH. For the SPP-QP-PE7 (IEC = 3.0 mmol $g^{-1}$), SPP-QP with IEC = 3.8 mmol $g^{-1}$ was used.


https://doi.org/10.1021/acsmaterialsau.1c00002
ACS Mater. Au 2021, 1, 81−88

hydrogen permeability of the SPP-QP-PE7 membrane. The ohmic resistance of the SPP-QP-PE7 cell was approximately 60 mΩ cm$^2$, which was higher than that (4 mΩ cm$^2$) obtained by the proton conductivity (0.335 S cm$^{-1}$; see Figure 4) and the membrane thickness (12 μm), probably due to the contact resistance with the catalyst layers. The SPP-QP-PE7 cell showed *IV* curves comparable to those of the bare SPP-QP cell. The ohmic resistance at OCV of the SPP-QP-PE7 and the bare SPP-QP cells at 30% RH was 0.36 and 0.31 Ω cm$^2$, respectively, which decreased as an increase in the current density as the product water back-diffused into the membranes. In the case of the bare SPP-QP cell, the ohmic resistance was approximately 0.12 Ω cm$^2$ (>0.6 A cm$^{-2}$), which was much lower than that (0.41 Ω cm$^2$) expected from the proton conductivity at 80 °C and 30% RH and the thickness and comparable to that (0.10 Ω cm$^2$) calculated from the proton conductivity at 80 °C and 40% RH and the thickness. The ohmic resistance of the SPP-QP-PE7 cell was ∼0.13 Ω cm$^2$ (>0.6 A cm$^{-2}$), comparable to that (0.13 Ω cm$^2$) obtained by the proton conductivity at 80 °C and 30% RH and the thickness, implying somewhat smaller water permeability of the SPP-QP-PE7 membrane due to the nonionic PE substrate. The maximum power density for the fuel cells ($H_2/O_2$) at 80 °C was 0.954 W cm$^{-2}$ for the SPP-QP cell and 0.943 W cm$^{-2}$ for the SPP-QP-PE7 cell at 100% RH, and 0.812 W cm$^{-2}$ for the SPP-QP cell and 0.758 W cm$^{-2}$ for the SPP-QP-PE7 cell at 30% RH, respectively (Figure S4).

The IR-free *IV* curves of the cells are replotted in Figure S5. The SPP-QP-PE7 cell showed a performance comparable with that of the SPP-QP cell at both 100 and 30% RH, suggesting a sufficient compatibility of the SPP-QP-PE7 membrane with the catalyst layers having a Nafion binder.

In the case of feeding air as the oxidant (Figure S6), the maximum current density decreased significantly at 30% RH. With increasing current density, the ohmic resistance decreased from 0.45 to 0.29 Ω cm$^2$ for SPP-QP-PE7 and from 0.39 to 0.22 Ω cm$^2$ for SPP-QP, which were higher than that with $O_2$ under the same operating conditions. As the gas utilization for the fuel cells with $O_2$ and air was constant (40%), the product water tended to be exhausted with an air flux rather than back-diffused into the membranes. Overall, the SPP-QP-PE7 membrane exhibited comparable or only slightly lower polarization curves compared with the bare SPP-QP membrane at high or low humidity and with $O_2$ or air.

Mechanical durability under practical conditions was evaluated via the USDOE protocol.[27] Briefly, wet (anode: 150% RH $H_2$, 2 L min$^{-1}$; cathode: 150% RH $N_2$, 2 L min$^{-1}$) and dry (anode: 0% RH $H_2$, 2 L min$^{-1}$; cathode: 0% RH $N_2$, 2 L min$^{-1}$) gases were alternately subjected to the fuel cells (80 °C) every 2 min, and $H_2$ crossover through the membrane was quantified by gas chromatography. Regarding the configuration of the SPP-QP-PE9 (2.55 mmol g$^{-1}$, 23 μm) cell, soft GDL (consisting of acetylene black, graphite, PTFE, without PTFE-bonded hard carbon fibers) was used, and a subgasket film (PPS) was utilized in the edge region of the MEA to decrease the stress onto the membrane.[24] As shown in Figure 7, The $H_2$ crossover percentage of the SPP-QP-PE9 cell was initially ∼0.001%, which was substantially lower than those of our previous SPK cell (∼0.012%) and Nafion cell (∼0.24%) with similar configuration.[24] The $H_2$ crossover percentage after 3850 cycles did not change, indicating that the SPP-QP-PE9 membrane was mechanically durable under the tested conditions.

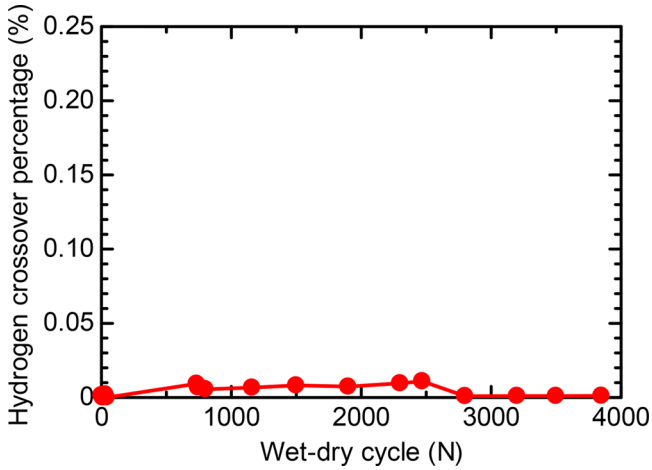


**Figure 7.** Hydrogen crossover percentage of the SPP-QP-PE9 (IEC = 2.6 mmol g$^{-1}$) cell (SPP-QP with IEC = 3.2 mmol g$^{-1}$ was used) during the humidity cycling test at 80 °C.

## CONCLUSIONS

We have successfully prepared new reinforced aromatic ionomer membranes (SPP-QP-PE), composed of a sulfonated polyphenylene (SPP-QP) and a porous polyethylene (PE) mechanical support layer, by the push coating method. The SPP-QP-PE membranes possessed a dense sandwich-like (triple-layer) (i.e., SPP-QP/SPP-QP + PE/SPP-QP) structure, whose (PE) pores were well-impregnated with SPP-QP throughout the membranes. The SPP-QP-PE (1.33 × 10$^{-9}$ cm$^3$ (STD) cm cm$^{-2}$ s$^{-1}$ cmHg$^{-1}$ for hydrogen, 3.90 × 10$^{-10}$ cm$^3$ (STD) cm cm$^{-2}$ s$^{-1}$ cmHg$^{-1}$ for oxygen, at 80 °C and 90% RH) membrane exhibited permeability coefficients comparable to those of the bare SPP-QP (1.46 × 10$^{-9}$ cm$^3$ (STD) cm cm$^{-2}$ s$^{-1}$ cmHg$^{-1}$ for hydrogen, 4.72 × 10$^{-10}$ cm$^3$ (STD) cm cm$^{-2}$ s$^{-1}$ cmHg$^{-1}$ for oxygen, at 80 °C and 90% RH), which were much lower than those (7.35 × 10$^{-9}$ cm$^3$ (STD) cm cm$^{-2}$ s$^{-1}$ cmHg$^{-1}$ for hydrogen, 3.15 × 10$^{-9}$ cm$^3$ (STD) cm cm$^{-2}$ s$^{-1}$ cmHg$^{-1}$ for oxygen, at 80 °C and 90% RH) for the perfluorinated Nafion membrane. The use of higher IEC SPP-QP was effective for the improvement in proton conductivity of the SPP-QP-PE7 (e.g., 5.67 mS cm$^{-1}$ at 80 °C and 20% RH), leading to the high fuel cell performance at low humidified conditions (e.g., at 80 °C and 30% RH). The flexible PE substrate improved the mechanical toughness of the membranes; the elongation at break of the SPP-QP-PE7 was as much as 134%, which was higher by a factor of 7.1 compared to that of the bare SPP-QP membrane (19%). Consequently, the SPP-QP-PE9 membrane was durable in the wet−dry cycle test for at least 3850 wet−dry cycles under the practical conditions (USDOE protocol).

## ASSOCIATED CONTENT

### Supporting Information

The Supporting Information is available free of charge at https://pubs.acs.org/doi/10.1021/acsmaterialsau.1c00002.

Measurements, water uptake, and proton conductivity of the membranes as a function of the IEC values, proton conductivity of the membranes as a function of relative humidity, LSVs of the fuel cells, IR-included $H_2/O_2$ *I*/*V* and *I*/*W* curves of the fuel cells, IR-free $H_2/O_2$ polarization curves and ohmic resistances of the fuel


https://doi.org/10.1021/acsmaterialsau.1c00002
ACS Mater. Au 2021, 1, 81−88

cells, IR-included $H_2$/air polarization curves and ohmic resistances of the fuel cells (PDF)

## AUTHOR INFORMATION


### Corresponding Author

**Kenji Miyatake** − *Clean Energy Research Center and Fuel Cell Nanomaterials Center, University of Yamanashi, Kofu, Yamanashi 400-8510, Japan; Department of Applied Chemistry, and Research Institute for Science and Engineering, Waseda University, Tokyo 169-8555, Japan;* orcid.org/0000-0001-5713-2635; Email: miyatake@yamanashi.ac.jp

### Authors

**Junpei Miyake** − *Clean Energy Research Center, University of Yamanashi, Kofu, Yamanashi 400-8510, Japan;* orcid.org/0000-0002-0689-061X

**Takayuki Watanabe** − *Interdisciplinary Graduate School of Medicine and Engineering, University of Yamanashi, Kofu, Yamanashi 400-8510, Japan*

**Haruhiko Shintani** − *Technology Division, Panasonic Corporation, Moriguchi 570-8501, Japan*

**Yasushi Sugawara** − *Appliances Company, Panasonic Corporation, Kusatsu 525-8520, Japan*

**Makoto Uchida** − *Fuel Cell Nanomaterials Center, University of Yamanashi, Kofu, Yamanashi 400-8510, Japan;* orcid.org/0000-0002-7847-3727

Complete contact information is available at: https://pubs.acs.org/10.1021/acsmaterialsau.1c00002


### Author Contributions

K.M. developed the intellectual concept, designed all the experiments, and supervised this research. J.M. and T.W. prepared the SPP-QP-PE membrane. T.W. performed the MEA fabrication and FC experiments. H.S. and Y.S. conducted the wet−dry cycling test. J.M., M.U., and K.M. analyzed all experimental data and wrote the paper.

### Notes

The authors declare no competing financial interest.

## ACKNOWLEDGMENTS

This work was partly supported by the Ministry of Education, Culture, Sports, Science and Technology (MEXT) Japan through a Grant-in-Aid for Scientific Research (KAKENHI JP18K04746, JP18H02030, and JP18H05515), by the New Energy and Industrial Technology Development Organization (NEDO), by Japan Science and Technology (JST) through SICORP, by JKA promotion funds from AUTORACE, and by thermal and electric energy technology foundation.

## REFERENCES


(1) Hammer, B. A. G.; Müllen, K. Dimensional Evolution of Polyphenylenes: Expanding in All Directions. *Chem. Rev.* **2016**, *116*, 2103−2140.

(2) Carrette, L.; Friedrich, K. A.; Stimming, U. Fuel Cells - Fundamentals and Applications. *Fuel Cells* **2001**, *1*, 5−39.

(3) Kusoglu, A.; Weber, A. Z. New Insights into Perfluorinated Sulfonic-Acid Ionomers. *Chem. Rev.* **2017**, *117*, 987−1104.

(4) Hickner, M. A.; Ghassemi, H.; Kim, Y. S.; Einsla, B. R.; McGrath, J. E. Alternative Polymer Systems for Proton Exchange Membranes (PEMs). *Chem. Rev.* **2004**, *104*, 4587−4612.

(5) Borup, R.; Meyers, J.; Pivovar, B.; Kim, Y. S.; Mukundan, R.; Garland, N.; Myers, D.; Wilson, M.; Garzon, F.; Wood, D.; Zelenay, P.; More, K.; Stroh, K.; Zawodzinski, T.; Boncella, J.; McGrath, J. E.; Inaba, M.; Miyatake, K.; Hori, M.; Ota, K.; Ogumi, Z.; Miyata, S.; Nishikata, A.; Siroma, Z.; Uchimoto, Y.; Yasuda, K.; Kimijima, K.; Iwashita, N. Scientific Aspects of Polymer Electrolyte Fuel Cell Durability and Degradation. *Chem. Rev.* **2007**, *107*, 3904−3951.

(6) Miyatake, K.; Chikashige, Y.; Higuchi, E.; Watanabe, M. Tuned Polymer Electrolyte Membranes Based on Aromatic Polyethers for Fuel Cell Applications. *J. Am. Chem. Soc.* **2007**, *129*, 3879−3887.

(7) Peckham, T. J.; Holdcroft, S. Structure-Morphology-Property Relationships of Non-Perfluorinated Proton-Conducting Membranes. *Adv. Mater.* **2010**, *22*, 4667−4690.

(8) Zhang, H.; Shen, P. K. Recent Development of Polymer Electrolyte Membranes for Fuel Cells. *Chem. Rev.* **2012**, *112*, 2780−2832.

(9) Kreuer, K. D. Ion Conducting Membranes for Fuel Cells and other Electrochemical Devices. *Chem. Mater.* **2014**, *26*, 361−380.

(10) Park, C. H.; Lee, S. Y.; Hwang, D. S.; Shin, D. W.; Cho, D. H.; Lee, K. H.; Kim, T.-W.; Kim, T.-W.; Lee, M.; Kim, D.-S.; Doherty, C. M.; Thornton, A. W.; Hill, A. J.; Guiver, M. D.; Lee, Y. M. Nanocrack-Regulated Self-Humidifying Membranes. *Nature* **2016**, *532*, 480−483.

(11) Lee, K.-S.; Spendelow, J. S.; Choe, Y.-K.; Fujimoto, C.; Kim, Y. S. An Operationally Flexible Fuel Cell Based on Quaternary Ammonium-Biphosphate Ion Pairs. *Nat. Energy* **2016**, *1*, 16120.

(12) Shin, D. W.; Guiver, M. D.; Lee, Y. M. Hydrocarbon-Based Polymer Electrolyte Membranes: Importance of Morphology on Ion Transport and Membrane Stability. *Chem. Rev.* **2017**, *117*, 4759−4805.

(13) Fujimoto, C. H.; Hickner, M. A.; Cornelius, C. J.; Loy, D. A. Ionomeric Poly(phenylene) Prepared by Diels-Alder Polymerization: Synthesis and Physical Properties of a Novel Polyelectrolyte. *Macromolecules* **2005**, *38*, 5010−5016.

(14) Skalski, T. J. G.; Britton, B.; Peckham, T. J.; Holdcroft, S. Structurally-Defined, Sulfo-Phenylated, Oligophenylenes and Polyphenylenes. *J. Am. Chem. Soc.* **2015**, *137*, 12223−12226.

(15) Adamski, M.; Skalski, T. J. G.; Britton, B.; Peckham, T. J.; Metzler, L.; Holdcroft, S. Highly Stable, Low Gas Crossover, Proton-Conducting Phenylated Polyphenylenes. *Angew. Chem.* **2017**, *129*, 9186−9189.

(16) Peressin, N.; Adamski, M.; Schibli, E. M.; Ye, E.; Frisken, B. J.; Holdcroft, S. Structure-Property Relationships in Sterically Congested Proton-Conducting Poly(phenylene)s: the Impact of Biphenyl Linearity. *Macromolecules* **2020**, *53*, 3119−3138.

(17) Miyake, J.; Taki, R.; Mochizuki, T.; Shimizu, R.; Akiyama, R.; Uchida, M.; Miyatake, K. Design of Flexible Polyphenylene Proton-conducting Membrane for Next-generation Fuel Cells. *Sci. Adv.* **2017**, *3*, No. eaao0476.

(18) Giancola, S.; Zatoń, M.; Reyes-Carmona, Á.; Dupont, M.; Donnadio, A.; Cavaliere, S.; Rozière, J.; Jones, D. J. Composite short side chain PFSA membranes for PEM water electrolysis. *J. Membr. Sci.* **2019**, *570*−*571*, 69−76.

(19) Bonnet, B.; Jones, D. J.; Rozière, J.; Tchicaya, L.; Alberti, G.; Casciola, M.; Massinelli, L.; Bauer, B.; Peraio, A.; Ramunni, E. Hybrid organic-inorganic membranes for a medium temperature fuel cell. *J. New Mat. Electrochem. Systems* **2000**, *3*, 87−92.

(20) Oh, K.-H.; Lee, D.; Choo, M.-J.; Park, K. H.; Jeon, S.; Hong, S. H.; Park, J.-K.; Choi, J. W. Enhanced Durability of Polymer Electrolyte Membrane Fuel Cells by Functionalized 2D Boron Nitride Nanoflakes. *ACS Appl. Mater. Interfaces* **2014**, *6*, 7751−7758.

(21) Zhang, T.; He, W.; Goldbach, J.; Mountz, D.; Yi, J. In situ proton exchange membrane fuel cell durability of poly(vinylidene fluoride)/polyelectrolyte blend Arkema M43 membrane. *J. Power Sources* **2011**, *196*, 1687−1693.

(22) Miyake, J.; Kusakabe, M.; Tsutsumida, A.; Miyatake, K. Remarkable Reinforcement Effect in Sulfonated Aromatic Polymers as Fuel Cell Membrane. *ACS Appl. Energy Mater.* **2018**, *1*, 1233−1238.

(23) Ikawa, M.; Yamada, T.; Matsui, H.; Minemawari, H.; Tsutsumi, J.; Horii, Y.; Chikamatsu, M.; Azumi, R.; Kumai, R.; Hasegawa, T.

Simple push coating of polymer thin-film transistors. *Nat. Commun.* **2012**, *3*, 1176.
(24) Ishikawa, H.; Teramoto, T.; Ueyama, Y.; Sugawara, Y.; Sakiyama, Y.; Kusakabe, M.; Miyatake, K.; Uchida, M. Use of a sub-gasket and soft gas diffusion layer to mitigate mechanical degradation of a hydrocarbon membrane for polymer electrolyte fuel cells in wet-dry cycling. *J. Power Sources* **2016**, *325*, 35−41.
(25) Yamauchi, M.; Tsuji, Y. Membrane-electrode-assembly and fuel cell. JP Patent Appl. 2011-4773582.
(26) Yamauchi, M.; Tsuji, Y. Membrane-electrode-assembly and fuel cell. U.S. Patent Appl. 0076592 A1, 2011.
(27) U.S. Department of Energy; https://www.energy.gov/ (accessed 2021-04-13).



https://doi.org/10.1021/acsmaterialsau.1c00002
*ACS Mater. Au* 2021, 1, 81−88